Impeded Electron Transfer From a Pathogenic FMN Domain Mutant of Methionine Synthase Reductase and Its Responsiveness to Flavin Supplementation[†]

Carmen G. Gherasim,[‡] Uzma Zaman,[‡,§] Ashraf Raza,[‡] and Ruma Banerjee*[,‡,||]

Biochemistry Department, University of Nebraska, Lincoln, Nebraska 68588-0664, International Center for Chemical and Biological Sciences, H.E.J Research Institute of Chemistry, University of Karachi, Karachi-75270, Pakistan, and Department of Biological Chemistry, University of Michigan, Ann Arbor, 48109-0606

Received May 7, 2008; Revised Manuscript Received October 7, 2008

ABSTRACT: Methionine synthase reductase (MSR) is a diflavin oxidoreductase that transfers electrons from NADPH to oxidized cobalamin and plays a vital role in repairing inactive cobalamin-dependent methionine synthase. MSR deficiency is a recessive genetic disorder affecting folate and methionine metabolism and is characterized by elevated levels of plasma homocysteine. In this study, we have examined the molecular basis of MSR dysfunction associated with a patient mutation, A129T, which is housed in the FMN binding domain and is adjacent to a cluster of conserved acidic residues found in diflavin oxidoreductases. We show that the substitution of alanine with threonine destabilizes FMN binding without affecting the NADPH coenzyme specificity or affinity, indicating that the mutation's effects may be confined to the FMN module. The A129T MSR mutant transfers electrons to ferricyanide as efficiently as wild type MSR but the rate of cytochrome c, 2,6-dichloroindophenol, and menadione reduction is decreased 10−15 fold. The mutant is depleted in FMN and reactivates methionine synthase with 8% of the efficiency of wild type MSR. Reconstitution of A129T MSR with FMN partially restores its ability to reduce cytochrome c and to reactivate methionine synthase. Hydrogen−deuterium exchange mass spectrometric studies localize changes in backbone amide exchange rates to peptides in the FMN-binding domain. Together, our results reveal that the primary biochemical penalty associated with the A129T MSR mutant is its lower FMN content, provide insights into the distinct roles of the FAD and FMN centers in human MSR for delivering electrons to various electron acceptors, and suggest that patients harboring the A129T mutation may be responsive to riboflavin therapy.

Methionine metabolism in mammals furnishes cells with three important metabolites, S-adenosylmethionine, needed for methylation reactions, glutathione, an important antioxidant, and taurine, an osmolyte. Homocysteine is a junction intermediate in this metabolic network and, at elevated levels, constitutes a risk factor for cardiovascular diseases, neural tube defects, and Alzheimer's disease (*1*−*3*). Homocysteine concentrations are kept low by the concerted actions of at least three enzymes: betaine homocysteine methyltransferase, methionine synthase, and cystathionine β-synthase. Impairments in the latter two enzymes and in the auxiliary protein that supports the activity of methionine synthase, i.e. methionine synthase reductase (MSR)[1], result in inborn errors of metabolism associated with severely elevated plasma homocysteine levels (*4, 5*). MSR is a dual flavoprotein oxidoreductase, which catalyzes the NADPH-dependent one-electron reduction of the cob(II)alamin cofactor formed occasionally during the catalytic cycle of methionine synthase. The latter is only one of two cobalamin-dependent enzymes found in mammals and catalyzes the transmethylation of homocysteine and methyltetrahydrofolate (CH_3-H_4folate) generating methionine and tetrahydrofolate (H_4folate) (*6*). The methyl transfer reaction occurs in two stages in which the cobalamin cofactor alternately accepts and then donates the methyl group (eqs 1 and 2) (*7*)

$$CH_3\text{-}H_4\text{folate} + \text{cob(I)alamin} \rightarrow H_4\text{folate} + \text{methylcob(III)alamin} \quad (1)$$

$$\text{methylcob(III)alamin} + \text{homocysteine} \rightarrow \text{cob(I)alamin} + \text{methionine} \quad (2)$$

Cob(I)alamin is an intermediate in this reaction and is labile to oxidation. It is estimated to escape once every ~2000 catalytic cycles (*8*). Over time, this would lead to accumulation of inactive methionine synthase were it not for the presence of an auxiliary repair system that regenerates the active enzyme in a reductive methylation reaction. This reactivation reaction requires *S*-adenosylmethionine for methyl group donation and MSR for delivery of electrons from NADPH to cob(II)alamin.

Initially identified through bioinformatic and genetic approaches, biochemical studies later demonstrated that MSR, a soluble monomeric protein with a molecular weight

[†] This work was supported by grants from the National Institutes of Health (DK64959 and 1P20RR17675).

* Corresponding author. Tel: (734)-615-5238, e-mail: rbanerje@umich.edu.

[‡] University of Nebraska, Lincoln.

[§] University of Karachi.

[||] University of Michigan.

[1] Abbreviations: MSR, methionine synthase reductase; DCIP, 2,6-dichloroindophenol; FAD_{sq} and FAD_{hq}, semiquinone and hydroquinone forms of FAD; FMN_{sq}, and FMN_{hq}, semiquinone and hydroquinone forms of FMN.

10.1021/bi8008328 CCC: $40.75
Published on Web 11/04/2008

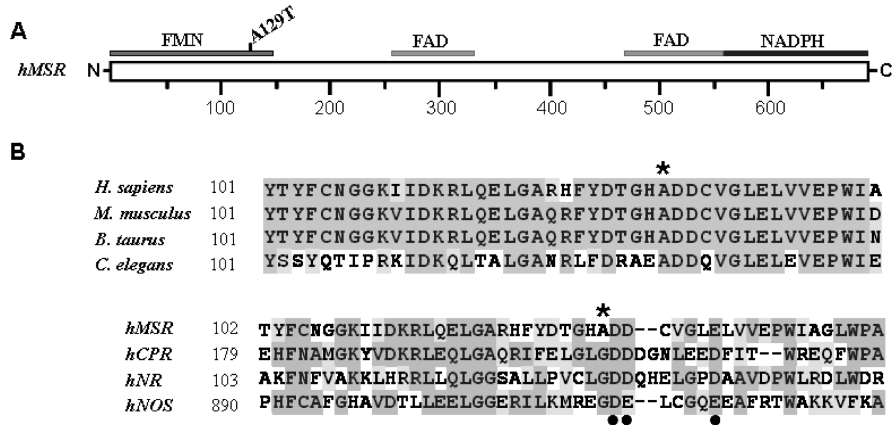

FIGURE 1: (A) Position of the A129T mutation in MSR relative to the FAD/NADPH and FMN binding domains. (B) Multiple sequence alignment of MSR homologues from other organisms and other diflavin oxidoreductases, in the region encompassing the mutated residue. The sequence alignment was prepared using BioEdit software using the sequence of MSR for the following species: *Homo sapiens* (NP_002445), *Mus musculus* (NP_766068), *Bos taurus* (AAY86763), *Caenorhabditis elegans* (Q17574), and cytochrome P450 reductase (NP_000932), novel reductase 1 (NP_055249), and neuronal nitric oxide synthase (NP_000611) respectively, all from *Homo sapiens*. The A129 residue, mutated in this study is represented by *, and the putative acidic cluster residues that are proximal to A129 in MSR are denoted by black dots.

of 78 kDa, sustains methionine synthase activity in vitro (*9*−*11*). A mouse model of MSR deficiency exhibits elevated levels of homocysteine and methyltetrahydrofolate and reduced methionine levels supporting the role of this enzyme in methionine synthase reactivation (*12*). Unlike the bacterial counterpart that is composed of two distinct proteins: flavodoxin and NADPH-ferredoxin oxidoreductase, MSR encompasses the FAD and FMN domains that have become fused in a single polypeptide (Figure 1A). This organization is also seen in other members of the diflavin oxidoreductase family of proteins which include cytochrome P450 reductase, nitric oxide synthase, and novel reductase 1 (*13*). The functions of these proteins depend on the two noncovalently bound flavin centers that mediate electron transfer from NADPH to cognate electron acceptors.

In addition to their physiological redox partners, flavin reductases can reduce small molecules such as ferricyanide, 2,6 dichloroindophenol (DCIP), 3-acetylpyridine ADP, and quinones, including menadione and doxorubicin. Interestingly, not all the acceptors receive electrons from the same flavin site, allowing dissection of the kinetic steps in the pathway of electron transfer (*14*). Characterization of the FMN-depleted cytochrome P450 reductase obtained by selective removal of the FMN prosthetic group, either by treatment with high ionic strength buffers or by site-directed mutagenesis of residues in the FMN binding site, established that the sequence of electron transfer in diflavin reductases is NADPH→FAD→FMN (*15, 16*). Moreover, these studies allowed assignment of the low and high potential flavins as FAD and FMN, respectively (*15*). Thus, reduced FMN is required to reduce physiological acceptors such as cytochrome P450s or surrogate electron acceptors such as DCIP, menadione, and cytochrome c whereas the FAD cofactor can directly transfer electrons to ferricyanide. Evidence for similar roles of the FAD and FMN cofactors in MSR derive both from studies on the thermodynamic properties of the flavins and the kinetic characterization of the reductive half-reactions (*17, 18*). The electron transfer in the reductive half-reaction follows a three-step process. First, reduction of MSR with NADPH results in the rapid formation of a charge-transfer complex followed by the slower reduction of FAD. Subsequently, the electrons are disproportionated between the flavins, a process controlled by the relative redox potentials of the FAD_{hq}/FMN_{ox}, FAD_{sq}/FMN_{sq}, and FAD_{ox}/FMN_{hq} couples. Finally, reduction by a second NADPH molecule generates a four-electron-reduced species FAD_{hq}/FMN_{hq} (*18*).

The crystal structures of cytochrome P450 reductase and nitric oxide synthase (*19*) revealed that the FMN-binding domain has a flavodoxin-like structure with a number of residues involved in stabilizing the noncovalently bound cofactor. In addition to residues stacking with the isoalloxazine rings, residues such as T88, T90, D208, N175, N182, H180, G143, and G141 (using the numbering for rat cytochrome P450 reductase) reside in the vicinity of the FMN cofactor and may be involved in hydrogen bonding interactions (*19*). Biochemical studies have identified two highly conserved clusters of acidic residues in the FMN binding domain of cytochrome P450 reductase, ^{207}Asp-Asp-Asp^{209} (cluster 1) and ^{213}Glu-Glu-Asp^{215} (cluster 2) that control its interactions with cytochrome P450 or cytochrome c (*20*). Two conserved acidic residues from cluster 1, D918 and E919 in neuronal nitric oxide synthase, D144 and E145 in the *Anabaena* flavodoxin, and D208 in cytochrome P450 reductase have been identified as key residues that regulate electron transfer to their acceptors (*20*−*22*). Interestingly, mutating these residues in rat cytochrome P450 reductase and in *Anabaena* flavodoxin inhibits electron transfer without affecting FMN binding whereas mutations in neuronal nitric oxide synthase destabilize FMN binding. Multiple sequence analyses predict that D130-D131 and E136 constitute the analogous acidic residues in human MSR (Figure 1B) with presumably similar roles and A129 is adjacent to this acidic cluster.

A number of mutations have been described in the MSR gene in homocystinuric patients belonging to the *cbl*E complementation group (*23, 24*). These defects are inherited as autosomal recessive disorders and are clinically characterized by presentation of hyperhomocysteinemia, hypomethionimia, and megaloblastic anemia. Treatment with hydroxocobalamin has been shown to be clinically efficient in some instances (*25*). Alternative dietary supplements used

to treat *cbl*E patients include folate and betaine (*26*). Although, mutations in MSR have been identified in both the FAD and FMN binding domains of the protein, nothing is known about the potential responsiveness of these mutants to riboflavin.

In this study, we have investigated the kinetic consequences of the A129T pathogenic mutation on flavin binding, overall protein conformation, and electron transfer to the physiological and to artificial electron acceptors. Our data reveal that the mutation results in an FMN-depleted protein with diminished reductive activities for type I electron acceptor such as cytochrome c, DCIP, and methionine synthase. This study provides biochemical insights into the basis of the A129T mutation's pathogenicity and suggests that riboflavin supplementation may be useful in some instances for treating homocystinuric patients with dysfunctional MSR.

EXPERIMENTAL PROCEDURES

Materials. Chemicals were purchased from Sigma unless stated otherwise. Restriction enzymes were purchased from Life Technologies and Fermentas while the oligonucleotides were purchased from Sigma Genosys. AdoMet 1,4-butanedisulfonate was a generous gift from Knoll Farmaceutici Spa (Milano, Italy). Glutathione Sepharose 4B, Superose 12 column, and 6-(*R,S*)-5-[$^{14}CH_3$]-H_4folate (barium salt, 55 mCi/mmol) were purchased from GE Health/Amersham Pharmacia. 6-(*R,S*)-CH_3-H_4folate (calcium salt) was obtained from Dr. Schirck's laboratory (Jona, Switzerland). The microbore C4 and C18 columns used for the hydrogen−deuterium exchange studies were purchased from MicroTech Scientific (Sunnyvale, CA). Methionine synthase was purified from porcine livers obtained from the slaughterhouse in Crete, NE. All solvents were HPLC grade.

Molecular Biology. The A129T site specific mutant was constructed using the expression vector pHOMSR for human MSR as template (*10*). The polymorphic background of MSR in this plasmid is I22/S175. Site-directed mutagenesis was performed using the QuickChange kit (Stratagene) and the following primers:

Sense: 5′-TATGACACTGGACATACCGATGACTGTGTAGGT-3′ and

Antisense: 5′-ACCTACACAGTCATCGGTATGTCCAGTGTCATA-3′.

The mutagenic codon specifying threonine is underlined. Following PCR amplification, a 0.6 kb *Bgl*II-*Kpn*I fragment containing the mutation was exchanged with the complementary fragment in the wild-type plasmid. The presence of the A129T mutation was confirmed by sequencing at the Genomics Core Facility (University of Nebraska, Lincoln). Mutant MSR was transformed into the *Escherichia coli* strain, BL21(DE3), for expression studies.

Expression and Purification of Wild-Type and A129T MSR. Wild-type and mutant MSR were expressed and purified using a previously reported protocol (*10*) with the following modifications. Limited proteolysis with thrombin was performed after removal of glutathione by extensive dialysis of the protein in 1X GST bind/wash buffer (1.47 mM KH_2PO_4, 4.3 mM Na_2HPO_4, 2.7 mM KCl, 137 mM NaCl). MSR was then separated from the GST tag by chromatography on a glutathione Sepharose 4B column and further purified by anion exchange chromatography on a MonoQ column. This purification procedure yielded 7 mg of mutant protein per liter of bacterial culture with a purity of >90% as judged by SDS-PAGE.

Quantitation of MSR-Bound Flavin. The FAD and FMN cofactors were released from wild-type and mutant protein by heating the samples at 95 °C for 5 min followed by rapid cooling on ice and centrifugation to remove precipitated protein. The flavin content was measured using an HPLC-based method described previously (*10*).

Steady-State Kinetic Analysis. Reduction of external electron acceptors was monitored directly for cytochrome c at 550 nm ($\varepsilon = 21$ mM^{-1} cm^{-1}) and DCIP at 600 nm ($\varepsilon = 20.6$ mM^{-1} cm^{-1}) or indirectly, for ferricyanide, menadione, and doxorubicin by measuring the extent of NADPH oxidation at 340 nm. All reactions were performed in 50 mM Tris pH 7.5, at 37 °C as described previously (*27*). The reactivation of methionine synthase by A129T MSR was determined using a previously described method (*10*).

Rapid Reaction Kinetics Experiments. The kinetics of flavin reduction was monitored under anaerobic conditions using an Applied Photophysics stopped-flow spectrophotometer housed in an anaerobic chamber. All experiments were performed at 25 °C in 50 mM potassium phosphate buffer (pH 7.0). Prior to the stopped flow experiments, proteins were treated with potassium ferricyanide to oxidize residual air-stable semiquinone that is present in MSR after purification. Excess ferricyanide was removed using PD-10 columns pre-equilibrated with anaerobic 50 mM phosphate buffer (pH 7.0). The final concentration of wild-type and mutant proteins after mixing was 7−11 μM and a 70-fold excess of NADPH was employed. For the dependence of flavin reduction on NADPH concentration, a range of 25−750 μM NADPH was used. The kinetic traces were biphasic (over 5 s) and were best fit to a double exponential function described by eq 3 where C_1 and C_2 are the relative amplitudes of the two phases and k_{obs1} and k_{obs2} are the observed rate constants for the fast and slow phases, respectively.

$$A = C_1 e^{-k\text{obs}1t} + C_2 e^{-k\text{obs}2t} + b \quad (3)$$

Isothermal Titration Calorimetry. All calorimetric binding experiments were performed using a VP-ITC microcalorimeter (1.44 mL cell volume) (Microcal, Inc., Northampton, MA). Protein samples were dialyzed overnight against 50 mM Tris-HCl pH 7.5, prior to being used in the titrations. The ligand and dialyzed proteins were filtered through 0.22 μm PVDF filters (Millipore) and degassed for 10 min at 20 °C with a ThermoVac sample degasser. The concentration of wild type and A129T MSR in these experiments was 30−50 μM as determined using the Bradford method and by absorbance at 454 nm (for wild-type MSR). $NADP^+$ (500−850 μM) was loaded in the syringe and added in 10 μL increments to the protein at 300 s intervals. The heats of binding were corrected for the heat dilution by subtracting the average heat associated with multiple injections of ligand following saturation of the binding sites. Experiments were performed in duplicate or triplicate, and the data were analyzed using the Microcal ORIGIN software using a single site binding model to determine the equilibrium association constant, K_A and the binding enthalpy, $\Delta H°$. The Gibbs free

Table 1: Kinetic Parameters for the Reduction of Various Acceptors by A129T and Wild-Type MSR

	A129T MSR		wild-type MSR	
substrate	k_{cat} (s^{-1})	K_M (M × 10^{-6})	k_{cat}[a] (s^{-1})	K_M[a] (M × 10^{-6})
ferricyanide	8.6 ± 0.45	630 ± 93	7.1 ± 0.2[a]	774 ± 53[a]
DCIP	0.058 ± 0.005	1.1 ± 0.08	0.67 ± 0.04[a]	3.8 ± 0.8[a]
menadione	0.13 ± 0.004	7.8 ± 1.4	1.61 ± 0.04[a]	18 ± 1.5[a]
doxorubicin	0.71 ± 0.051	137 ± 28	1.60 ± 0.06[a]	28.6 ± 3.3[a]
cytochrome c	0.16 ± 0.009	ND	3.1 ± 0.1	ND

[a] Values for wild-type MSR obtained from reference *27*; NADPH was used as electron donor.

energy of binding, $\Delta G°$, and the entropic contribution to the binding free energy, $-T\Delta S°$, were calculated using eqs 4 and 5.

$$\Delta G° = -RT \ln K_A \quad (4)$$

$$\Delta G° = \Delta H° - T\Delta S° \quad (5)$$

Hydrogen−Deuterium (H/D) Exchange Mass Spectrometry. Initial experiments with intact protein were performed to determine the extent of sequence coverage. For this, purified wild-type MSR (10 μg) in 100 mM ammonium phosphate buffer pH 2.5 was digested with pepsin (1:1 w/w) for 5 min on ice after prior removal by centrifugation of particulate matter associated with the protein solution. The peptic fragments were separated by HPLC and identified by tandem ESI-MS/MS, which yielded 63% sequence coverage. For H/D exchange studies, wild-type and A129T enzymes (10 μg) in 50 mM phosphate buffer pH 7.0 were diluted 10-fold in the exchange buffer prepared in D_2O (5 mM phosphate buffer, pD 7). The kinetics of hydrogen exchange were monitored from 10 s to 5 h, and the reaction was quenched with 0.5 M HCl to decrease the pH to 2.5. The quenched samples were immediately frozen in liquid nitrogen and stored at −80 °C until further use. After thawing, samples were digested with pepsin as described above. The loss of deuterium under the experimental conditions was corrected in the estimation of the final peptide mass using eq 6, where D is the adjusted deuterium

$$D = \frac{m - m_{100\%}}{m_{100\%} - m_{0\%}} \times N \quad (6)$$

incorporation, m is the observed mass at a given time, $m_{0\%}$ is the 0% or undeuterated control, $m_{100\%}$ is the fully deuterated control, and N is the total number of exchangeable amide hydrogens that does not include the N-terminal proton or proline residues. The $m_{0\%}$ was determined by diluting 10 μg of protein 10-fold in quench buffer, followed rapidly by the addition of an equal amount of exchange buffer, and the final mix was subjected to pepsin digestion. To obtain the $m_{100\%}$ value for fully deuterated MSR, 10 μg of the protein sample was incubated overnight at room temperature in 8 M guanidinium hydrochloride prepared in D_2O. Subsequently, the sample was diluted 10-fold with ammonium phosphate, pH 2.5, followed by pepsin digestion. The extent of deuterium incorporation into individual peptides was determined by LC/ESI-MS using the same conditions as previously reported with the following modification in the elution step (*28*). The peptic peptides were eluted from the C_{18} microbore column using a linear gradient from 2 to 60% acetonitrile (0.3% formic acid) over 27 min with a flow rate of 100 μL/min. The masses of the individual peptides were identified by ESI-MS on a quadrupole time-of-flight mass spectrometer (Applied Biosystems). MagTran software was used to calculate the centroid value for each peptide.

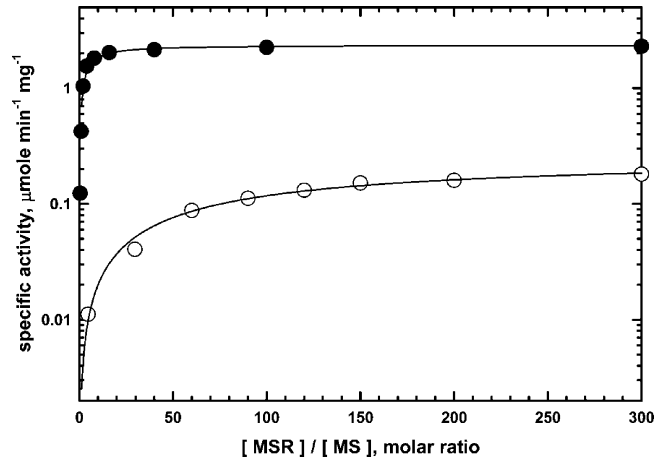

FIGURE 2: Activation of methionine synthase by A129T and wild-type MSR. The activity of methionine synthase was determined as described previously (*10*) at the indicated A129T (○) or wild-type (●) MSR:methionine synthase (MS) ratios.

RESULTS

Purification and Spectroscopic Properties of A129T MSR. The recombinant A129T mutant was purified using a protocol developed for wild-type MSR (*10*) and yielded 7 mg of protein per liter of culture. The UV−visible absorption spectrum of the mutant revealed a higher A_{280}/A_{454} ratio of 7.9 compared to 4.8 for wild-type MSR, indicating lower flavin content in the mutant. This was confirmed by HPLC analysis, which revealed that the mutant contained the full complement of FAD (1.07 ± 0.04) but only 0.2 ± 0.05 mol of FMN/mol of protein.

Electron Transfer from A129T MSR to Exogenous Electron Acceptors. The kinetic properties of the A129T mutant are compared with the values for wild-type MSR (*27*) in Table 1. The reductase activity of mutant MSR was determined with the protein as isolated, i.e., containing substoichiometric FMN. The mutation impaired electron transfer to cytochrome c, DCIP, and menadione exhibiting an ∼10−15-fold decrease in the respective turnover numbers and a more modest ∼2−3-fold decrease in the K_M for these acceptors. In contrast, reduction of potassium ferricyanide was essentially unaffected, indicating that the mutant retains its ability to receive electrons from NADPH and that reduced FAD is the source of electrons for ferricyanide. These data are consistent with cytochrome c, DCIP, and menadione accepting electrons from the FMN domain of MSR, in analogy with other diflavin reductases (*15*).

Reactivation of Methionine Synthase. Next, we compared the efficacy of the A129T mutant relative to wild-type MSR

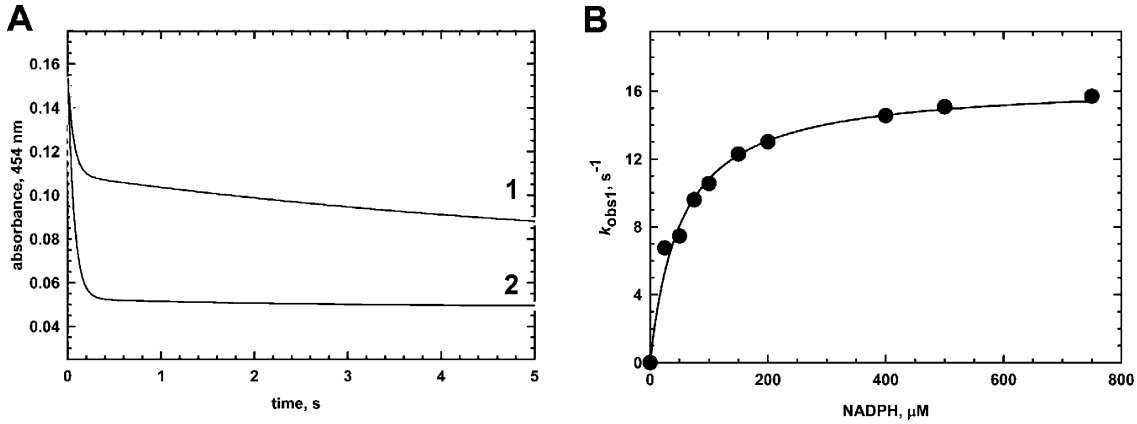

FIGURE 3: Kinetics of flavin reduction in wild type and A129T MSR determined by stopped-flow spectroscopy. (A) Single-wavelength absorption experiments for the reduction of 7 μM wild-type (**1**) and 11.27 μM A129T MSR (**2**) with 500 μM NADPH were followed at 454 nm under anaerobic conditions in 50 mM potassium phosphate, pH 7.0, at 25 °C. Biphasic absorption traces for the reduction of MSR proteins were obtained by fitting the data in panels A with a double exponential equation as described under Experimental Procedures. The black line running through each experimental trace (shown in gray) represents the best fit using eq 3. Panel B shows the dependence of k_{obs1} for the A129T MSR reaction on NADPH concentration.

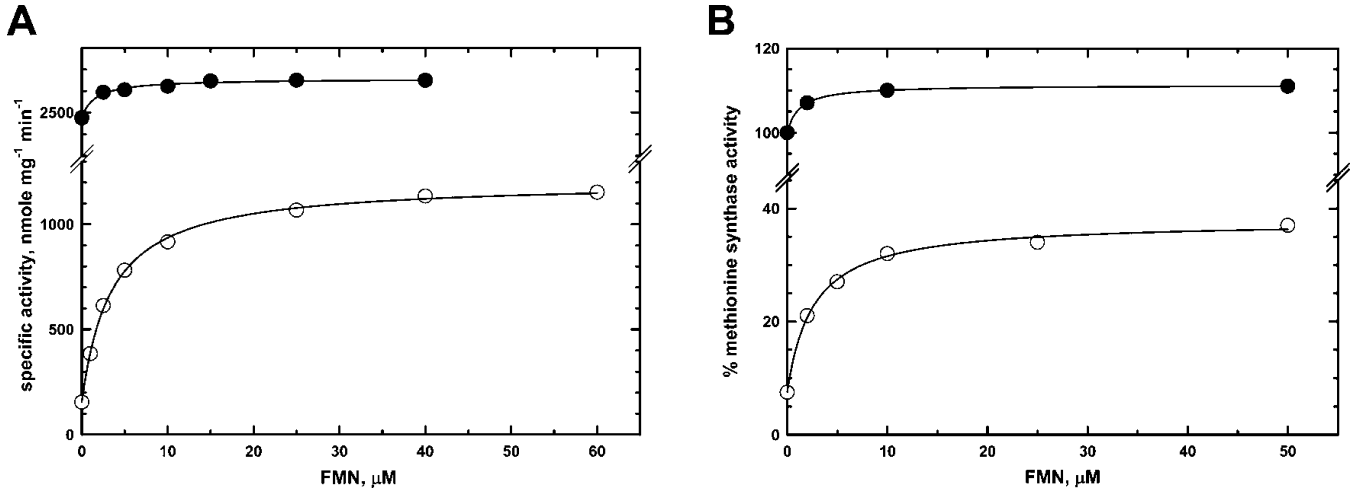

FIGURE 4: Effect of exogenous FMN on MSR activity. (A) Cytochrome c reductase activity of wild-type (●) and A129T (○) MSR in the absence or presence of various FMN concentrations were measured by incubating the respective proteins in the assay mixture containing 50 mM Tris pH 7.5, 60 μM cytochrome c, and 100 μM NADPH and 0−60 μM FMN in a final volume of 1 mL. Reactions were initiated by addition of NADPH, and the initial velocities were monitored at 37 °C. (B) Methionine synthase activity determined in the presence or absence of exogenous FMN when wild-type (●) or A129T (○) MSR were used as a reactivating protein partner.

in supporting the activity of methionine synthase. A 14-fold lower specific activity for methionine synthase was observed even when a 100-fold excess of A129T MSR over methionine synthase was used compared to a 3-fold excess of wild-type MSR (Figure 2). The results are consistent with FMN being critical for the relay of electrons to methionine synthase and/or the A129T mutation disrupting the interaction between the redox partners.

Stopped-Flow Analysis of Flavin Reduction. FMN-depleted or partially replete nNOS mutants have been shown to increase the rate of FAD reduction (*21*). To test whether this is also true for A129T MSR, the flavin reduction rates in the mutant and wild-type proteins were compared. Experiments were performed under pseudo-first-order conditions using a 70-fold excess of NADPH, and flavin reduction was monitored at 454 nm (Figure 3). Stopped-flow kinetic traces were best fit to a biphasic process where the first phase (k_{obs1}) can be attributed to FAD reduction by NADPH and the second phase (k_{obs2}) to electron transfer to the FMN site with the formation of E•($FADH_2$/FMN; $FADH^{\bullet}$/$FMNH^{\bullet}$; FAD/$FMNH_2$). The apparent rate constants for wild-type MSR (Figure 3A) were 17.1 s^{-1} (k_{obs1}) and 0.15 s^{-1} (k_{obs2}), similar to values reported previously (*18, 29*). The apparent rate constants for flavin reduction in the A129T mutant (Figure 3A) were 16.8 s^{-1} (k_{obs1}) and 0.42 s^{-1} (k_{obs2}). Thus, the rate constant for the second phase in the mutant is 2.8 times higher than in wild-type MSR. The greater amplitude of the first phase for the A129T versus wild-type MSR likely reflects the greater accumulation of the $FADH_2$ species since it cannot be quantitatively converted to the $FADH^{\bullet}$/$FMNH^{\bullet}$ or $FMNH_2$ forms due to the lower occupancy at the FMN site. By extension, the low amplitude associated with the second phase in the A129T mutant is consistent with only a small fraction of the protein being in the FMN reduced state.

The observed rate constant of flavin reduction for the A129T MSR mutant was monitored as a function of NADPH concentration and exhibited a hyperbolic dependence on the coenzyme concentration (Figure 3B). The maximal rate constant for flavin reduction in the A129T mutant, 16.5 s^{-1} (k_{lim}), is lower than the value (24.8 s^{-1}) determined for wild-type MSR (*18*).

$NADP^+$ Binding to A129T MSR. An unresolved question in the sequence of mechanistic steps of flavin reduction is

Table 2: Comparison of the Thermodynamic Parameters for Binding of $NADP^+$ to Wild-Type MSR and the A129T Mutant[a]

protein	N	K_D, μM	$\Delta H°$, kcal/mol	$T\Delta S°$, kcal/mol	$\Delta G°$, kcal/mol
wild-type MSR	1.07 ± 0.13	54 ± 5.3	-7.9 ± 0.8	-2.3 ± 0.7	-5.6 ± 0.49
A129T MSR	1.15 ± 0.19	32 ± 2.9	-5.1 ± 0.25	0.93 ± 0.09	-6.0 ± 0.14

[a] The experiments ($n = 3$) were performed at 20 °C, and the values represent mean ± SD.

the stage at which the release of $NADP^+$ takes place. The expulsion of the oxidized coenzyme impacts the rate of flavin reduction in cytochrome P450 reductase (*30*). Although the A129T mutation did not affect the K_M for NADPH (K_M = 2.8 μM versus 2.6 μM for wild-type MSR) or the specificity of the protein for NADPH versus NADH in the cytochrome c reduction assay (not shown), we tested to see if the mutation affects the dissociation constant for $NADP^+$ (Table 2 and Supporting Information Figure 2). The energetics of $NADP^+$ binding to wild-type and A129T MSR were monitored by isothermal titration calorimetry. Binding of $NADP^+$ to A129T MSR is accompanied by a $\Delta G°$ of -5.6 ± 0.49 kcal/mol compared to -6.0 ± 0.14 kcal/mol in wild-type MSR. A 1.7-fold lower K_D value was obtained for the A129T mutant along with small differences in the other thermodynamic parameters. Hence, the A129T mutant has a slightly higher affinity for the oxidized coenzyme compared to wild-type MSR.

Effect of FMN Reconstitution on Electron Transfer. The lower reduction efficiency of the A129T MSR mutant can be partially attributed to its FMN depletion. When exposed to varying concentrations of FMN, the A129T mutant exhibited a partial improvement in the efficacy of cytochrome c reduction reaching 45% of the maximal value obtained with wild-type MSR (Figure 4A). Similar effects were observed when A129T MSR was tested for its ability to reactivate methionine synthase in the presence of 2.5−50 μM FMN (Figure 4B). Wild-type MSR exhibited a 10% increase in activity in the presence of exogenous FMN in both the cytochrome c reduction and methionine synthase reactivation assays, indicating some loss of FMN even from the wild-type protein. Thus, the A129T mutation is partially responsive to FMN supplementation and in this respect, resembles mutants in neuronal nitric oxide synthase, cytochrome P450, and cytochrome P450 BM3 in which FMN binding has been disrupted (*16, 21, 31*).

H/D Exchange Studies. H/D exchange mass spectrometric studies were undertaken to potentially identify peptides that exhibit differences in exchange kinetics as a consequence of the missense mutation in the FMN domain. Of the ~60 peptides representing 63% sequence coverage (Supporting Information Figure 1), that were identified in both the wild-type and the A129T mutant of MSR, a significant difference in the deuterium incorporation was observed only in seven peptides representing three nonoverlapping fragments, which exhibited an increase in deuterium incorporation of 1.5−2 Da per peptide (Figure 5A−C). The three peptides, spanning residues 36−55, 56−75, and 86−102, map to the putative FMN binding domain (Figure 6A). A peptide spanning the A129 residue was not detected. We note that the restricted sequence coverage obtained in this study limits our insights into locations of other conformational differences that could exist between the mutant and wild-type MSR since they could have been missed in the peptides that were not identified.

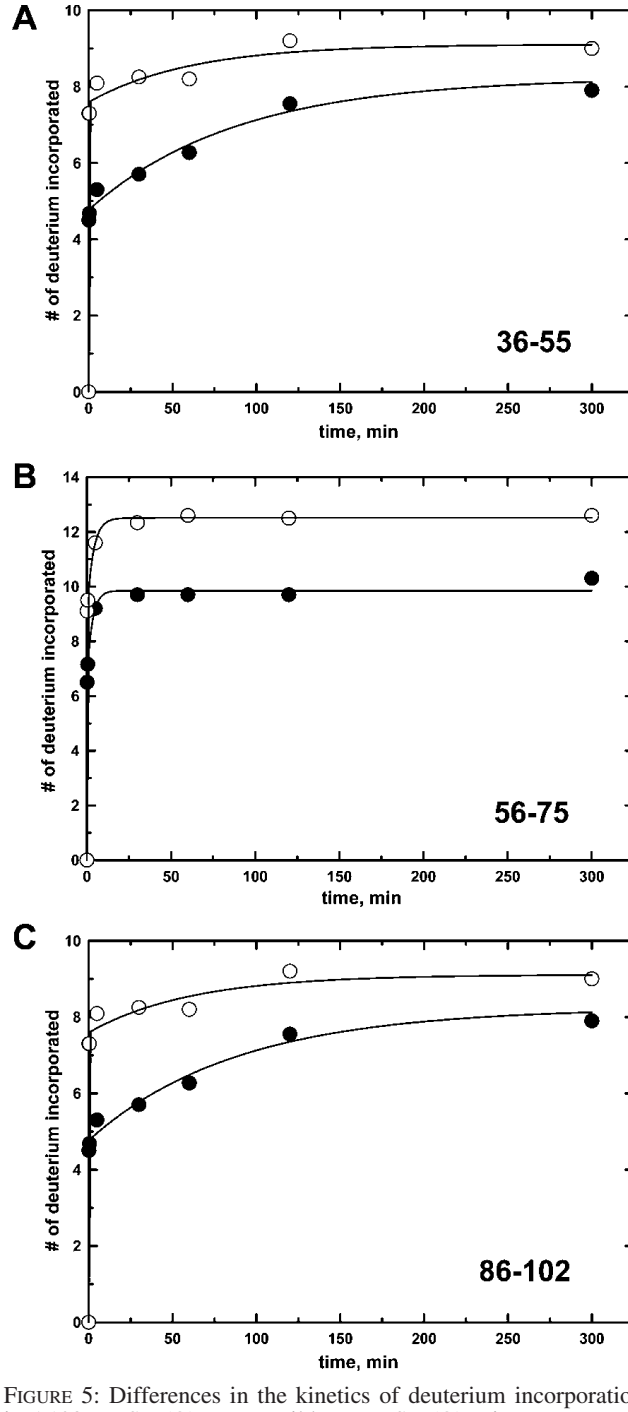

FIGURE 5: Differences in the kinetics of deuterium incorporation in A129T MSR (○) versus wild-type MSR (●). Time courses are shown for peptide 36−55 (A), peptide 56−75 (B), and peptide 86−102 (C).

DISCUSSION

The A129T mutation in MSR was described in a homocystinuric patient belonging to the *cbl*E class of inborn errors of folate/cobalamin metabolism. The patient is heterozygous for this mutation and harbors a three base pair deletion, V54del (c.160delGTT), on the second MSR-

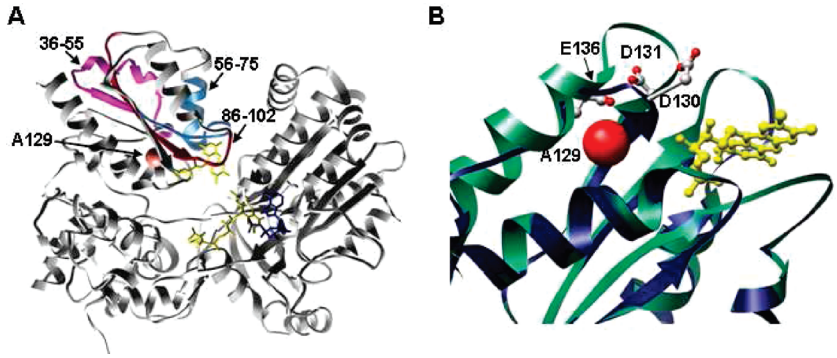

FIGURE 6: (A). Map of peptides that exhibit differences in H/D exchange kinetics in the A129T mutant compared to wild-type MSR. Peptides identified by H/D exchange studies map to the FMN binding domain of MSR and are shown in blue (36−55), magenta (56−75), and red (86−102), and the A129 residue is shown in surface representation. The modeled structure for the FMN binding domain was created using the alignment mode of the SWISS-MODEL program (www.swissmodel.expasy.org/SWISSMODEL.html) with cytochrome P450 reductase as template. (B) Location of the A129T mutation in the modeled structure of the FMN-binding domain of MSR. Superimposition of cytochrome P450 reductase (PDB file 1AMO) and a modeled structure of the FMN domain of human MSR showing the location of A129 relative to the FMN cofactor. The putative acidic cluster residues in MSR and the FMN cofactor are shown in ball and stick representation.

encoding allele (*23*). Methionine synthase activity in cultured fibroblasts derived from this patient (WG1384) was the lowest in a panel of *cbl*E cell lines that we had previously tested and exhibited an ∼10−14 fold lower activity compared to control fibroblasts (*32*). In contrast to a prior assignment of the A129T mutant as being in the linker domain between the FAD and FMN domains (*23*), multiple sequence alignment of diflavin oxidoreductases revealed that A129 resides in the FMN binding domain of MSR, adjacent to a cluster of acidic residues (Figures 1 and 6B). Our study demonstrates that the A129T mutation destabilizes FMN binding, with immediate consequences on the activity of MSR as tested with its physiological redox partner, methionine synthase, and with surrogate electron acceptors. Supplementation with exogenous FMN partially rescued the reductase activity of the mutant. The inability of the A129T mutant protein to fully restore methionine synthase activity even at high FMN concentrations indicates that the mutation elicits additional effects besides decreasing the FMN content. For instance, the mutation also appears to impair the interaction between the FMN binding domain and its redox partner as evidenced by the significantly higher MSR:methionine synthase ratio needed for maximal methionine synthase activity, which is 14-fold lower than with wild-type MSR (Figure 2). The crystal structure of rat CPR (*19*) revealed a relatively high degree of similarity with other members of the diflavin family of proteins including nNOS (*33*), human CPR (*34*), and P450BM3 (*35*). A recently reported crystal structure of the FAD−NADPH binding domain of MSR confirmed the expectation that key structural and functional elements are highly conserved in this class of proteins (*36*). A modeled structure for the full-length MSR places the A129 residue at the tip of a β-strand in the immediate vicinity of the FMN cofactor (Figure 6A). This residue is not conserved in other diflavin reductases where the alanine is replaced with a glycine (Figure 1B). Destabilization of FMN binding in the A129T mutation is consistent with A129 being located in the proximity of FMN. The introduction of a side chain hydroxyl group in the A129T mutant could potentially introduce a hydrogen bond to D130 or disrupt the interactions with the neighboring β strand perturbing the FMN environment.

Approximately 30% of patients with disease-causing mutations that affect vitamin-dependent enzymes respond to high doses of the relevant vitamin (*37*). The mutant phenotype typically results from a decreased binding affinity for the cofactor or decreased stability of the mutant protein (*38*). Homocysteine-dependent transmethylation and transsulfuration pathways converge at a vitamin-rich metabolic juncture. Studies on mutations in methionine synthase, cystathionine β-synthase, and methylenetetrahydrofolate reductase indicate that treatment with vitamins B_{12}, B_6, and riboflavin can partially alleviate the phenotype associated with these genetic defects (*39*). Following riboflavin supplementation, an accumulation of riboflavin and flavocoenzymes occurs via a transporter (with a K_M of 12 ± 1.3 μM in liver cells), suggesting that at high riboflavin doses, a significant reconstitution of A129T MSR/methionine synthase activity may be achieved (*40*). Patients with mutations in MSR are generally treated with B_{12}, folate, or betaine (*41, 42*). Our data provide biochemical evidence for the potential utility of riboflavin treatment for homocystinuric patients with MSR deficiency.

SUPPORTING INFORMATION AVAILABLE

Supplementary Figures 1 and 2 are available free of charge via the Internet at http://pubs.acs.org.

REFERENCES

1. Mills, J. L., McPartlin, J. M., Kirke, P. N., Lee, Y. J., Conley, M. R., Weir, D. G., and Scott, J. M. (1995) Homocysteine metabolism in pregnancies complicated by neural-tube defects. *Lancet 345*, 149–151.
2. Clarke, R., Smith, A. D., Jobst, K. A., Refsum, H., Sutton, L., and Ueland, P. M. (1998) Folate, vitamin B12, and serum total homocysteine levels in confirmed Alzheimer disease. *Arch Neurol 55*, 1449–1455.
3. Refsum, H., Ueland, P. M., Nygard, O., and Vollset, S. E. (1998) Homocysteine and Cardiovascular Disease. *Annu. Rev. Med. 49*, 31–62.
4. Rosenblatt, D. S. (2001) *Inborn errors of folate and cobalamin metabolism*, Cambridge University Press, Cambridge.
5. Finkelstein, J. D. (2006) Inborn errors of sulfur-containing amino acid metabolism. *J. Nutr. 136*, 1750S–1754S.
6. Matthews, R. G. (2001) Cobalamin-dependent methyltransferases. *Acc. Chem. Res.* 34.
7. Banerjee, R. V., and Matthews, R. G. (1990) Cobalamin-dependent methionine synthase. *FASEB J. 4*, 1450–1459.
8. Drummond, J., Huang, S., Blumenthal, R. M., and Matthews, R. G. (1993) Assignment of enzymatic function to specific protein regions

of cobalamin-dependent methionine synthase from *Escherichia coli*. *Biochemistry 32*, 9290–9295.
9. Leclerc, D., Wilson, A., Dumas, R., Gafuik, C., Song, D., Watkins, D., Heng, H. H. Q., Rommens, J. M., Scherer, S. W., Rosenblatt, D. S., and Gravel, R. A. (1998) Cloning and mapping of a cDNA for methionine synthase reductase, a flavoprotein defective in patients with homocystinuria. *Proc. Natl. Acad. Sci. U.S.A. 95*, 3059–3064.
10. Olteanu, H., and Banerjee, R. (2001) Human methionine synthase reductase, a soluble P-450 reductase-like dual flavoprotein, is sufficient for NADPH-dependent methionine synthase activation. *J. Biol. Chem. 276*, 35558–35563.
11. Yamada, K., Gravel, R. A., Toraya, T., and Matthews, R. G. (2006) Human methionine synthase reductase is a molecular chaperone for human methionine synthase. *Proc. Natl. Acad. Sci. U.S.A. 103*, 9476–9481.
12. Elmore, C. L., Wu, X., Leclerc, D., Watson, E. D., Bottiglieri, T., Krupenko, N. I., Krupenko, S. A., Cross, J. C., Rozen, R., Gravel, R. A., and Matthews, R. G. (2007) Metabolic derangement of methionine and folate metabolism in mice deficient in methionine synthase reductase. *Mol. Genet. Metab. 91*, 85–97.
13. Porter, T. D., and Kasper, C. B. (1986) NADPH-cytochrome P-450 oxidoreductase: flavin mononucleotide and flavin adenine dinucleotide domains evolved from different flavoproteins. *Biochemistry 25*, 1682–1687.
14. Vermilion, J. L., Ballou, D. P., Massey, V., and Coon, M. J. (1981) Separate roles for FMN and FAD in catalysis by liver microsomal NADPH-cytochrome P-450 reductase. *J. Biol. Chem. 256*, 266–277.
15. Vermilion, J. L., and Coon, M. J. (1978) Identification of the high and low potential flavins of liver microsomal NADPH-cytochrome P-450 reductase. *J. Biol. Chem. 253*, 8812–8819.
16. Shen, A. L., Porter, T. D., Wilson, T. E., and Kasper, C. B. (1989) Structural analysis of the FMN binding domain of NADPH-cytochrome P-450 oxidoreductase by site-directed mutagenesis. *J. Biol. Chem. 264*, 7584–7589.
17. Wolthers, K. R., Basran, J., Munro, A. W., and Scrutton, N. S. (2003) Molecular dissection of human methionine synthase reductase: determination of the flavin redox potentials in full-length enzyme and isolated flavin-binding domains. *Biochemistry 42*, 3911–3920.
18. Wolthers, K. R., and Scrutton, N. S. (2004) Electron transfer in human methionine synthase reductase studied by stopped-flow spectrophotometry. *Biochemistry 43*, 490–500.
19. Wang, M., Roberts, D. L., Paschke, R., Shea, T. M., Masters, B. S., and Kim, J. J. (1997) Three-dimensional structure of NADPH-cytochrome P450 reductase: prototype for FMN- and FAD-containing enzymes. *Proc. Natl. Acad. Sci. U.S.A. 94*, 8411–8416.
20. Shen, A. L., and Kasper, C. B. (1995) Role of acidic residues in the interaction of NADPH-cytochrome P450 oxidoreductase with cytochrome P450 and cytochrome c. *J. Biol. Chem. 270*, 27475–27480.
21. Adak, S., Ghosh, S., Abu-Soud, H. M., and Stuehr, D. J. (1999) Role of reductase domain cluster 1 acidic residues in neuronal nitric-oxide synthase. Characterization of the FMN-free enzyme. *J. Biol. Chem. 274*, 22313–22320.
22. Jenkins, C. M., Genzor, C. G., Fillat, M. F., Waterman, M. R., and Gomez-Moreno, C. (1997) Negatively charged anabaena flavodoxin residues (Asp144 and Glu145) are important for reconstitution of cytochrome P450 17alpha-hydroxylase activity. *J. Biol. Chem. 272*, 22509–22513.
23. Wilson, A., Leclerc, D., Rosenblatt, D. S., and Gravel, R. A. (1999) Molecular basis for methionine synthase reductase deficiency in patients belonging to the cblE complementation group of disorders in folate/cobalamin metabolism. *Hum. Mol. Genet. 8* 2009–2016.
24. Vilaseca, M. A., Vilarinho, L., Zavadakova, P., Vela, E., Cleto, E., Pineda, M., Coimbra, E., Suormala, T., Fowler, B., and Kozich, V. (2003) CblE type of homocystinuria: mild clinical phenotype in two patients homozygous for a novel mutation in the MTRR gene. *J. Inherit. Metab. Dis. 26*, 361–369.
25. Rosenblatt, D. S., and Cooper, B. A. (1987) Inherited disorders of vitamin B12 metabolism. *Blood Rev. 1*, 177–182.
26. Muller, P., Horneff, G., and Hennermann, J. B. (2007) [A rare inborn error of intracellular processing of cobalamine presenting with microcephalus and megaloblastic anemia: a report of 3 children]. *Klin. Padiatr. 219*, 361–367.
27. Olteanu, H., Munson, T., and Banerjee, R. (2002) Differences in the efficiency of reductive activation of methionine synthase and exogenous electron acceptors between the common polymorphic variants of human methionine synthase reductase. *Biochemistry 41*, 13378–13385.
28. Sen, S., Yu, J., Yamanishi, M., Schellhorn, D., and Banerjee, R. (2005) Mapping Peptides Correlated with Transmission of Intrasteric Inhibition and Allosteric Activation in Human Cystathionine β-Synthase. *Biochemistry 44*, 14210–14216.
29. Olteanu, H., Wolthers, K. R., Munro, A. W., Scrutton, N. S., and Banerjee, R. (2004) Kinetic and thermodynamic characterization of the common polymorphic variants of human methionine synthase reductase. *Biochemistry 43*, 1988–1997.
30. Knight, K., and Scrutton, N. S. (2002) Stopped-flow kinetic studies of electron transfer in the reductase domain of neuronal nitric oxide synthase: re-evaluation of the kinetic mechanism reveals new enzyme intermediates and variation with cytochrome P450 reductase. *Biochem. J. 367*, 19–30.
31. Klein, M. L., and Fulco, A. J. (1993) Critical residues involved in FMN binding and catalytic activity in cytochrome P450BM-3. *J. Biol. Chem. 268*, 7553–7561.
32. Gulati, S., Chen, Z., Brody, L. C., Rosenblatt, D. S., and Banerjee, R. (1997) Defects in auxiliary redox proteins lead to functional methionine synthase deficiency. *J. Biol. Chem. 272*, 19171–19175.
33. Zhang, J., Martasek, P., Paschke, R., Shea, T., Siler Masters, B. S., and Kim, J. J. (2001) Crystal structure of the FAD/NADPH-binding domain of rat neuronal nitric-oxide synthase. Comparisons with NADPH-cytochrome P450 oxidoreductase. *J. Biol. Chem. 276*, 37506–37513.
34. Zhao, Q., Modi, S., Smith, G., Paine, M., McDonagh, P. D., Wolf, C. R., Tew, D., Lian, L. Y., Roberts, G. C., and Driessen, H. P. (1999) Crystal structure of the FMN-binding domain of human cytochrome P450 reductase at 1.93 A resolution. *Protein Sci. 8*, 298–306.
35. Sevrioukova, I. F., Li, H., Zhang, H., Peterson, J. A., and Poulos, T. L. (1999) Structure of a cytochrome P450-redox partner electron-transfer complex. *Proc. Natl. Acad. Sci. U.S.A. 96*, 1863–1868.
36. Wolthers, K. R., Lou, X., Toogood, H. S., Leys, D., and Scrutton, N. S. (2007) Mechanism of coenzyme binding to human methionine synthase reductase revealed through the crystal structure of the FNR-like module and isothermal titration calorimetry. *Biochemistry 46*, 11833–11844.
37. Mudd, S. H., Skovby, F., Levy, H. L., Pettigrew, K. D., Wilcken, B., Pyeritz, R. E., Andria, G., Boers, G. H., Bromberg, I. L., Cerone, R., et al. (1985) The natural history of homocystinuria due to cystathionine beta-synthase deficiency. *Am. J. Hum. Genet. 37*, 1–31.
38. Ames, B. N., Elson-Schwab, I., and Silver, E. A. (2002) High-dose vitamin therapy stimulates variant enzymes with decreased coenzyme binding affinity (increased K(m)): relevance to genetic disease and polymorphisms. *Am. J. Clin. Nutr. 75*, 616–658.
39. Kim, Y. J., and Rosenberg, L. E. (1974) On the mechanism of pyridoxine responsive homocystinuria. II. Properties of normal and mutant cystathionine beta-synthase from cultured fibroblasts. *Proc. Natl. Acad. Sci. U.S.A. 71*, 4821–4825.
40. Aw, T. Y., Jones, D. P., and McCormick, D. B. (1983) Uptake of riboflavin by isolated rat liver cells. *J. Nutr. 113*, 1249–1254.
41. Rosenblatt, D. S., Thomas, I. T., Watkins, D., Cooper, B. A., and Erbe, R. W. (1987) Vitamin B12 responsive homocystinuria and megaloblastic anemia: heterogeneity in methylcobalamin deficiency. *Am. J. Med. Genet. 26*, 377–383.
42. Ogier de Baulny, H., Gerard, M., Saudubray, J. M., and Zittoun, J. (1998) Remethylation defects: guidelines for clinical diagnosis and treatment. *Eur. J. Pediatr. 157* (2), S77–83.

BI8008328